Chinese Journal of Polar Science, Vol. 20, No. 2, 135 - 150, December 2009

Subdivision of petrologic type of unequilibrated ordinary chondrites from Antarctica

Jiang Yun(蒋云) and Hsu Weibiao(徐伟彪)
Laboratory for Lunar and Planetary Science, Purple Mountain Observatory, Chinese Academy of Sciences, Nanjing 210008, China

Received October 23, 2009

Abstract We report results of petrologic and mineralogical studies of 25 unequilibrated ordinary chondrites (19 Chinese Antarctic meteorites) using electron microprobe, scanning electron microscopy (SEM) and energy-dispersive X-ray spectrometry (EDS) techniques. With increasing degree of thermal metamorphism, chemical zoning of olivine was erased; plessite was transformed into intergrowths of coarser-grained kamacite and Ni-rich metal; Cr exsolved from ferroan olivine, produced needle-like crystals and coarsened into equant chromite grains; and feldspar crystallized during devitrification of glass and recrystallization of matrix. These features can help to identify different metamorphic grades. Based on the scheme by Sears *et al.* (1982), we subdivided type 3 Chinese Antarctic ordinary chondrites into petrologic type 3.3 to 4 (3 type 3.3, 3 type 3.4, 1 type 3.5, 2 type 3.6, 2 type 3.7, 5 type 3.8, 3 type 4). This classification scheme is a quite effective way to subdivide Antarctic meteorites. Additionally, we propose to revise the chemical groups of GRV 020032 and GRV 020104 to L and H, respectively.
Key words Antarctica, UOCs, thermal metamorphism, olivine, petrologic type.

1 Introduction

The petrologic type of primitive meteorites helps to reveal thermal metamorphism process and aqueous alteration history on their parent bodies. Van Schmus and Wood (1967)[1] first introduced the concept of petrologic type and grouped chondrites into 6 types. Petrologic types 3—6 reflect increasing degree of thermal metamorphism, whereas types 1 and 2 are used to designate meteorites that experienced different degrees of aqueous alteration. Type 3 chondrites, which suffered the least thermal metamorphism and the lowest aqueous alteration, are also called unequilibrated chondrites.

Sears *et al.* (1980)[2] first used thermoluminescence (TL) sensitivity as a strong indicator of metamorphic grade to subdivide type 3 into ten finer divisions: types 3.0 through 3.9. The TL sensitivity is dependent on the degree to which feldspar crystallizes out of primary chondrule glass and matrix in response to thermal metamorphism[3]. The criteria used for classification of petrologic types also include many other parameters, such as the water and carbon content[1, 4], the amount of primordial ^{36}Ar[5], the composition of opaque matrix and matrix olivine[6], as well as some parameters discovered recently, including Cr distribution in ferroan olivine[7], the chemical compositions of spinel group minerals[8], and the petrologic characteristics of Fe-Ni metal[9].

So far, TL sensitivity has been proven to be the most useful parameter to subdivide unequilibrated chondrites. However, this scheme is not practical in classification of Chinese Antarctic meteorites because most specimens have masses less than 1 g. In this work, we performed petrologic and mineralogical studies of 25 unequilibrated ordinary chondrites (UOCs) on thin or thick sections. We found that Fe-Ni metal texture, Cr exsolution in olivine, the matrix recrystallization and the abundance of secondary feldspar are good indicators of petrologic types of UOCs. Furthermore, we analyzed the composition of olivine and low-Ca pyroxene grains in all samples and applied the classification scheme proposed by Sears *et al* (1982) to subdivide petrologic types of 25 UOCs[10]. This method was proved to be useful in Antarctic meteorites classification[11].

2 Samples and experimental methods

We investigated polished thin or thick sections of 19 Antarctic meteorites collected by Chinese polar expeditions. 6 other UOCs were also included for comparison. A list of the samples analyzed in this study is given in Table 1.

Back-scattered electron (BSE) imaging and mineral analyses were obtained using the Hitachi S-3400N II scanning electron microscope (SEM) equipped with energy-dispersive X-ray spectrometry (EDS). Mineral chemical analyses were performed with the JEOL 8100 electron microprobe at China University of Geosciences. The operating conditions are 15 kV accelerating voltage and 20 nA beam current. Peak and background counting times are 10 s and 5 s for most elements, respectively. Natural and synthetic standards were used, and all data were reduced by ZAF procedure.

3 Results

3.1 Petrography

3.1.1 Fe-Ni metal textures

According to Kimura[9], there are three kinds of petrographic occurrences of Fe-Ni metal in ordinary chondrites: within chondrules, around chondrules and in the matrix. They are called chondrule interior metal, chondrule surface metal and isolated matrix metal, respectively. Chondrule interior metal is generally spherical in shape and 10—50 μm in diameter, whereas the latter two are irregularly shaped and much larger up to 100 μm in size.

In Semarkona (LL3.01), chondrules commonly contain metal spherules of kamacite and sub-micrometer Ni-rich metal (Fig. 1a). This metal was interpreted to be a plessitic intergrowth of kamacite and tetrataenite by Reisener and Goldstein[13]. In type 3.2—4.0 chondrites, Fe-Ni metal in chondrule interiors are much coarser-grained and do not show the plessitic intergrowth like that of Semarkona (Fig. 1b, 1c and 1d). In Krymka (LL3.2), a few Ni-rich metal grains are several micrometers (Fig. 1b), and most are around

Table 1. List of the samples in order of increasing petrologic type as determined in this work

Sample	Group[#]	Group[&]	Type	Type[¥]	Shock	Weathering	Find/Fall	Year
Semarkona	LL		3.01[@]		S2[£]	–	fall	1940
Krymka	LL		3.2		S3[£]	–	fall	1946
GRV 020035	L		3	3.3	S2	W2	find	2002
GRV 020032	LL	L	3	3.3	S2	W1	find	2002
GRV 020006	L		3	3.3	S2	W1	find	2002
Sharps	H		3.4		S3[£]	–	fall	1921
Chainpur	LL		3.4		S1[£]	–	fall	1907
GRV 020011	L		3	3.4	S2	W2	find	2002
GRV 020137	L		3	3.4	S2	W1	find	2003
GRV 020104	LL	H	3	3.4	S2	W1	find	2003
GRV 020169	L		3	3.5	S2	W1	find	2003
GRV 052191	H		3	3.6	S3	W3	find	2006
GRV 050009	H		3	3.6	S2	W1	find	2006
Julesburg	L		3.6		S3[$]		find	1983
Dimmitt	H		3.7				find	1942/1981
GRV 050016	H		3	3.7	S1	W1	find	2006
GRV 052722	H		3	3.7	S2	W2	find	2006
GRV 020034	LL		3	3.8	S2	W1	find	2002
GRV 020054	H		3	3.8	S4	W1	find	2003
GRV 020105	LL		3	3.8	S1	W2	find	2003
GRV 022921	H		3	3.8	S2	W2	find	2006
GRV 020036	LL		3	3.8	S2	W1	find	2002
GRV 022455	L		3	4	S4	W1	find	2003
GRV 021528	H		3	4	S1	W2	find	2003
GRV 022410	H		3	4	S2	W2	find	2006

–: showing no significant signs of weathering; # previous chemical group classification; & revised chemical group in this paper; @ petrologic type determined by [9]; ¥ classification results in this paper; £ quoted from [7]; $ quoted from [12].

15 μm. In GRV 020032, the grain size of Ni-rich metal is up to 40 μm (Fig. 1d). However, chondrule surface metal and isolated matrix metal in all samples are generally associated with troilite and do not show plessitic intergrowth textures. In addition, tiny inclusions of chromite and phosphate, less than a few micrometers, are commonly observed in metal spherules of chondrules in type 3.2—4.0 chondrites (Fig. 1d). Zanda[14] explained that Cr, P, Si, dissolved in metal grains of type 3.0 chondrites, get oxidized to form chromite, phosphates and silica due to weak metamorphism.

3.1.2 Cr exsolution features in olivine

Cr distribution in olivine of type II chondrules is different among ordinary chondrites with different petrologic types. In Semarkona (LL3.01), olivine grains in type II chondrules are Cr-rich (0.5 wt% Cr_2O_3), and show core-to-rim Cr zoning consistent with igneous fractionation[7]. In Krymka (LL3.2), olivine grains commonly show streaks of Cr-rich exsolution oriented along crystallographic axes (as indicated by crystal faces). We observed two kinds of streaks: sub-parallel (Fig. 2a) and parallel (Fig. 2b). Both of them are needle-like grains < 50 nm wide and up to 15 μm long, showing a strong Cr peak on EDS spectra. In type ≥3.3 chondrites, olivine grains in type II chondrules are uniformly low in Cr and are surrounded by a thin Cr-rich rim (Fig. 2c and 2d). Moreover, olivine cores contain scattered equant chromite grains (Fig. 2d). All Antarctic UOCs in this study show Cr-distribution patterns similar to those of type ≥3.3 chondrites. However, it should be noted here that not every olivine grain in type II chondrule presents this exsolution feature.

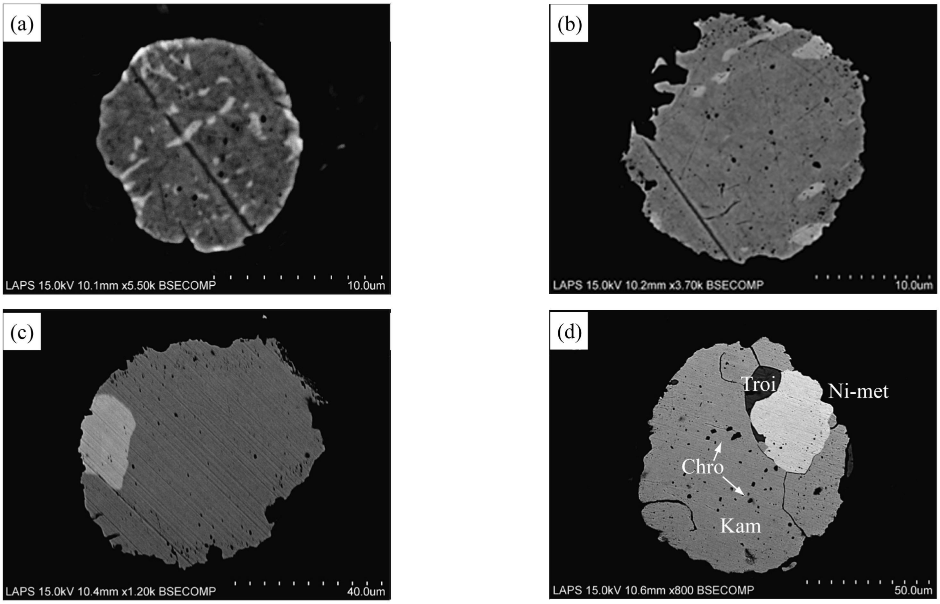

Fig. 1 Backscattered electron (BSE) images of chondrule interior metal. a) A fine-grained plessitic intergrowth of kamacite and sub-micrometer Ni-rich metal in Semarkona (LL3.01). b) A coarse-grained intergrowth of kamacite and micrometer Ni-rich metal in Krymka (LL3.2). c) A metal spherule consisting of kamacite and coarse-grained Ni-rich metal in GRV 020035 (L3.3). d) A metal spherule with tiny inclusions of chromite in GRV 020032 (LL3.3). Kam: kamacite; Ni-met: Ni-rich metal; Chro: chromite; Troi: troilite.

3.1.3 Matrix and secondary feldspar grains

Numerous studies of matrix were done to identify a series of changes in optical properties, mineralogy, and degree of chemical equilibration due to thermal metamorphism[6,7,15]. Furthermore, development of secondary feldspar in the matrix is responsible for the increase in blue cathodoluminescence (CL) as a function of metamorphic grade[3]. We examined the matrix of all samples under the scanning electron microscope and found that with increasing petrologic type, the abundance and grain size of secondary feldspar increase (Fig. 3, Table 2).

In Semarkona (LL3.01), the matrix mineral grain is extremely fine and contains numerous sub-micrometer grains of sulfide and Fe-Ni metal (Fig. 3a), consistent with the observation by Nagahara[15]. In Krymka (LL3.2), the matrix experienced mild thermal metamorphism with grains slightly coarser than Semarkona (Fig. 3b). As the recrystallized

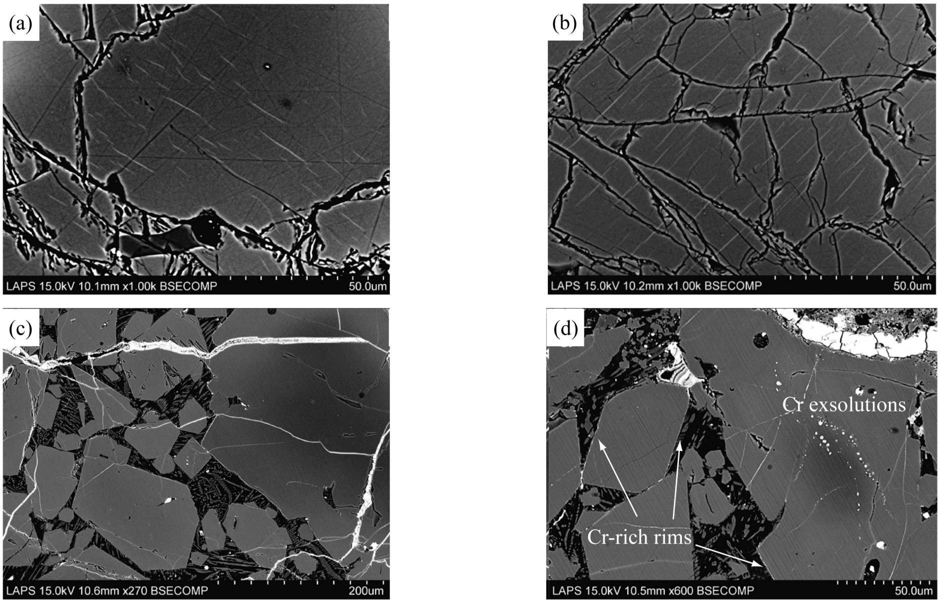

Fig. 2 BSE images of a) numerous sub-parallel streaks of Cr-rich exsolutions oriented along crystallographic axes of the olivine grain in Krymka; b) parallel streaks of Cr-rich exsolutions in another chondrule of Krymka; c) olivine grains are surrounded by a Cr-rich rim in GRV 020169; d) Cr-rich rims and Cr-rich exsolution products in the core of an olivine in GRV 020169.

grains in matrix becomes more abundant, the remaining opaque matrix becomes coarser, less friable, and increasingly depleted in minute metallic Fe-Ni metal and sulfide grains[6]. The matrices of GRV 020035 (L3.3), GRV 020032 (L3.3) and GRV 020006 (L3.3) are finer grained than that of Chainpur (Fig. 3c-f), which is a type 3.4 UOC. GRV 020032 and GRV 020006 are classified as type 3.3. In addition, we did not observe any secondary feldspar grains in the matrices of UOC with a petrologic type ⩽3.3 (Fig. 3a-e).

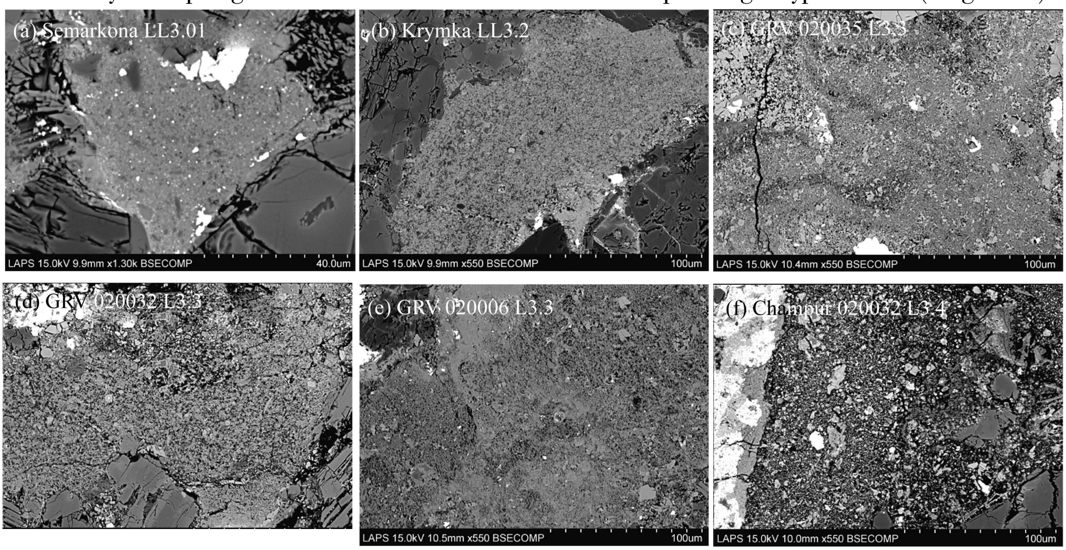

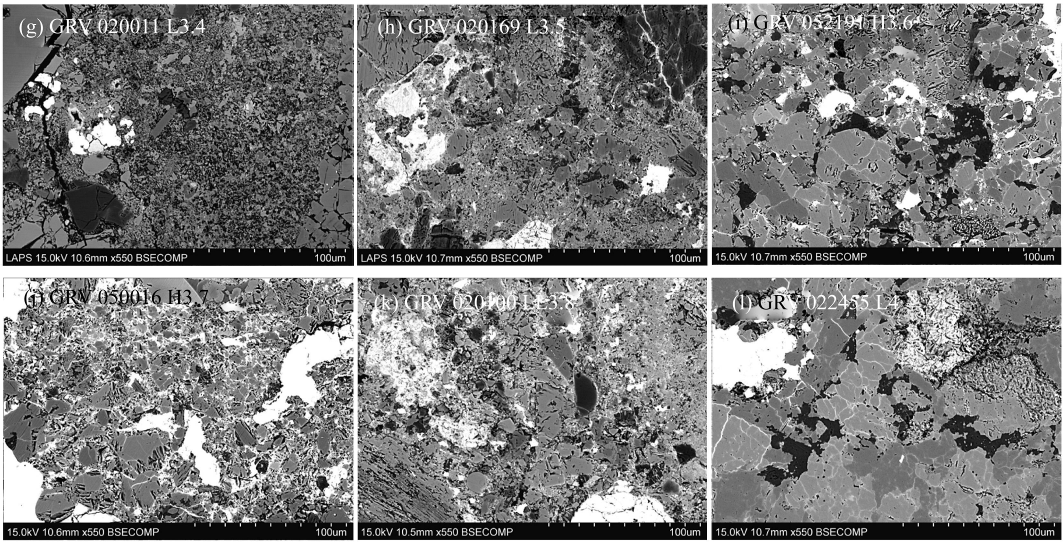

Fig 3 BSE images of matrices of petrologic type 3.01 (Semarkona) to type 4 (GRV 022455). In Semarkona, the matrix consists of extremely fine grained silicates, sulfides and Fe-Ni metal. With increasing thermal metamorphism, the matrix mineral grains are larger and the secondary albite nucleates and grows. In GRV 022455 (L4), the matrix is completely recrystallized.

Table 2 The features of the matrix and feldspar grain of some representative samples

Sample	Type	Matrix grain size	Feldspar grain
Semarkona	3.01	extremely fine grained	no
Krymka	3.2	very fine grained	no
GRV 020035	3.3	fine grained	no
GRV 020032	3.3	fine grained	no
GRV 020006	3.3	fine grained	no
Sharps	3.4	less fine grained	no
Chainpur	3.4	less fine grained	few, up to 5 μm
GRV 020011	3.4	less fine grained	few, up to 6 μm
GRV 020137	3.4	less fine grained	some, up to 10 μm
GRV 020104	3.4	less fine grained	some, up to 8 μm
GRV 020169	3.5	less coarse grained	some, up to 10 μm
GRV 052191	3.6	coarse grained	many, up to 20 μm
GRV 050009	3.6	coarse grained	many, up to 10 μm
Julesburg	3.6	coarse grained	some, up to 10 μm
GRV 050016	3.7	coarse grained	some, up to 10 μm
GRV 052722	3.7	coarse grained	many, up to 10 μm
GRV 020105	3.8	coarse grained	some, up to 12 μm
GRV 020036	3.8	coarse grained	some, up to 6 μm
GRV 022455	4	very coarse grained	many, up to 20 μm
GRV 022410	4	coarse grained	some, up to 8 μm

In type 3.4 UOCs, matrices become less fine-grained (Fig 3f, g) and characteristics of secondary feldspar grains are complicated. No feldspar grains were observed in Sharps, while a few grains up to 6 μm were found in Chainpur and GRV 020011. However, GRV 020137 and GRV 020104 contain some feldspar grains in matrices. Above petrologic type~3.5, matrix becomes more coarse-grained and feldspar grains are commonly present (Fig. 3h-l). The grain size of matrix is coarse to very coarse and feldspar is up to 20 μm. But there is no good correlation between the petrologic type and the abundance and grain size of feldspar in matrix between types 3.5—4.0.

3.2 Mineral chemistry

In each specimen, 80—120 olivine and pyroxene grains (> 15 μm in size) were analyzed by energy-dispersive X-ray spectrometry, using a very similar grain-selection method as described by Dodd[4]. Points were selected by traversing 500 μm steps along and 1000 μm apart. Smaller intervals were used for small samples. If there was no silicate grain at a point, or if there was a visible imperfection (inclusion, crack, or grain boundary) at the point, the sample was moved as much as 20 μm to reach a silicate grain[4]. For zoned grains, we analyzed the core and the rim, respectively. EDS Results of olivine and low-ca pyroxene grains in all samples are listed in Table 3.

Table 3. EDS Results of all samples

Sample	Group	Type	Ol(Fa)				Px(Fs)			
			Mean	CoV ©	Range	no#	Mean	CoV	Range	no
Semarkona	LL	3.01	12.4	57.1	0.8-33.4	74	11.5	62.8	1.2-29.1	34
Krymka	LL	3.2	15.3	63.9	0.4-41.3	70	11.6	70.5	1.6-31.9	70
GRV 020035	L	3.3	19.5	58.6	0.1-38.6	85	9.6	80.5	0.2-31.2	72
GRV 020032	L	3.3	20.1	57.1	1.7-37.6	73	9.3	87.3	1.0-29.8	70
GRV 020006	L	3.3	19.8	52.2	0.6-38.9	72	12.7	79.2	0.9-37.0	68
Sharps	H	3.4	16.3	56.9	0.5-36.7	76	8.5	75.1	0.8-22.1	60
Chainpur	LL	3.4	14.1	51.5	0.1-33.8	76	7.5	89.2	1.2-26.9	48
GRV 020011	L	3.4	21.3	51.2	0.5-36.7	72	11.6	67.4	1.2-31.7	64
GRV 020137	L	3.4	21.3	51.7	0.5-33.1	72	11.7	66.4	0.1-32.3	68
GRV 020104	H	3.4	19.3	53.3	0.6-33.9	72	13.2	56.5	1.0-24.5	72
GRV 020169	L	3.5	22.9	43.0	2.7-36.5	72	15.3	69.9	0.8-45.2	64
GRV 052191	H	3.6	18.6	31.0	0.9-41.0	52	17.0	21.8	4.2-29.5	52
GRV 050009	H	3.6	17.0	31.0	1.4-21.7	72	15.5	33.4	2.3-23.4	70
Julesburg	L	3.6	21.5	31.8	3.1-37.3	72	12.1	53.7	1.7-26.2	40
Dimmitt	H	3.6	17.9	39.8	0.8-26.9	72	14.4	46.0	1.9-29.3	55
GRV 050016	H	3.7	20.3	28.8	2.1-30.6	70	14.2	36.6	2.2-20.0	54
GRV 052722	H	3.7	20.4	27.6	1.6-28.8	72	13.0	56.8	2.5-30.5	40
GRV 020034	LL	3.8	27.3	18.3	6.8-29.9	52	20.0	25.3	7.8-26.1	40
GRV 020054	H	3.8	19.3	18.3	4.5-32.3	52	16.2	24.1	6.3-20.9	40
GRV 020105	LL	3.8	27.0	17.9	1.6-37.0	100	15.0	45.4	3.4-22.8	50
GRV 022921	H	3.8	19.1	12.8	7.0-23.7	52	15.6	19.5	2.3-17.1	40
GRV 020036	LL	3.8	27.6	11.8	5.0-28.6	52	15.3	46.5	2.5-31.5	50
GRV 022455	L	4	24.8	2.8	23.9-28.2	52	19.2	13.9	11.9-28.6	40
GRV 021528	H	4	19.9	2.6	18.6-21.9	52	19.7	19.5	3.6-26.1	40
GRV 022410	H	4	20.9	2.3	18.9-21.4	56	17.1	24.3	7.2-21.1	50

©: coefficient of variation (percent standard deviation); #: number of points analyzed

Chemical group results are based on the classification scheme by Van Schmus and Wood[1]. As olivine composition is not a reliable indicator for UOC with a low petrologic type (< 3.5)[16], we measured the mean size of all chondrules through the whole section using scanning electron microscope and calculated the model abundance of metal based on the BSE image (Table 4). According to Weisburg[16], the mean chondrule size (μm) and metal abundance (vol%) are 300, 700, 900 and 8, 4, 2 for H, L, LL respectively. Therefore, we group GRV 020035, GRV 020032, GRV 020006, GRV 020011, GRV 020137 and GRV 020104 into L, L, L, L, L, H respectively. Among them, GRV 020032 (L) and GRV 020104 (H) are different from their previous reports (LL). The chemical group results of other UOCs (type≥3.5), including Julesburg and Dimmitt, are consistent with their previous results.

Table 4. The mean chondrule size and metal abundance of UOCs

Sample	Chondrule size (um)	Metal abundance (vol%)	Chemical group
GRV 020035	607	4.1	L
GRV 020032	674	5.1	L
GRV 020006	696	5.3	L
GRV 020011	-	4.8	L
GRV 020137	-	5.6	L
GRV 020104	452	8.5	H

-: not measured

We analyzed the most Mg-rich and Fe-rich olivine and pyroxene grains in every sample using electron microprobe (Table 5 and 6).

Olivine compositional variation is a strong indicator of metamorphic grade (Fig. 4). Sears[10] compared olivine heterogeneity with TL sensitivity and proposed a scheme to subdivide the petrologic type of UOCs based on the coefficient of variation (CoV, defined by Scott, 1984 as the standard deviation of mol% Fa or Fs expressed as a percentage of the mean). Based on this definition, results of petrologic types of samples are presented in table 3. It should be noted that this definition is not sensitive for petrologic types between 3.0 and 3.4 (Fig. 4). Those UOCs of type 3.0-3.4 in table 3, with CoV value more than 50, are subdivided according to other parameters, including Fe-Ni metal features, Cr-exsolution features in olivine as well as matrix and secondary feldspar features. With the CoV being 31.8, Julesburg is subdivided into type 3.6, consistent with previous study[12]. As for Dimmitt, it consists of (in vol. %) 40% H4 and H5 chondrite clasts, 3% impact melt rock clasts, 0.5% shocked H chondrite clasts, 1.5% exotic clasts (including carbonaceous and LL5 chondrites), and 55% gas-rich matrix[17]. Based on the CoV value 39.8, Dimmitt belongs to type 3.6, slightly different from previous type 3.7[17]. However, Bischoff[18] pointed out that the CoV value has no real meaning for a sub-classification of chondritic breccias. In GRV 022455, GRV 021528 and GRV 022410, their olivine grains are almost equilibrated with CoV values of 1.3-2.8, corresponding to PMD values 1.0—2.2. Dodd[4] defined ordinary chondrites with the percent mean deviation of FeO measured in olivine (PMD-ol) less than 5% to be type 4. Therefore, we classify these three ordinary chondrites into type 4, though their pyroxenes are still quite heterogeneous in composition (table 3).

Table 5. Electron microprobe data (wt%) of the most Mg-rich and Fe-rich olivine grains in every sample

	Semarkona		Krymka		GRV 020035		GRV 020032		GRV 020006		Sharps		Chainpur		GRV 020011	
Na_2O	-	0.10	-	0.01	-	-	0.01	0.02	-	0.04	0.03	0.03	0.01	0.04	-	0.03
K_2O	-	0.01	0.02	0.01	-	0.02	0.01	-	0.01	0.01	-	-	0.02	-	-	-
Cr_2O_3	0.27	0.38	0.09	0.30	0.04	0.03	0.13	0.02	0.10	-	0.04	0.02	0.05	0.06	0.09	0.03
MgO	55.85	32.44	55.82	27.00	56.70	29.62	54.63	31.24	55.41	30.33	55.37	30.61	56.12	32.01	57.11	32.38
CaO	0.32	0.28	0.58	0.20	0.20	0.01	0.48	0.02	0.38	-	0.64	0.11	1.22	0.09	0.55	0.03
MnO	0.01	0.84	0.01	0.50	0.16	0.51	0.04	0.39	-	0.52	-	0.40	-	0.33	-	0.46
Al_2O_3	0.11	0.05	0.25	0.10	0.04	0.05	0.19	0.06	0.26	0.05	0.53	0.07	0.12	0.03	0.26	0.03
TiO_2	0.08	0.05	0.08	0.10	0.02	0.05	0.13	0.05	0.04	0.03	0.11	0.04	0.06	0.03	0.10	0.01
FeO	0.91	29.20	0.89	37.10	0.23	32.62	2.44	31.04	0.56	32.63	0.73	32.68	0.46	30.45	0.46	30.68
SiO_2	41.85	36.62	42.60	34.95	42.91	36.60	42.01	36.65	42.41	36.40	42.72	36.38	41.53	36.74	41.41	36.40
Total	99.39	99.95	100.32	100.27	100.30	99.50	100.08	99.48	99.17	100.02	100.17	100.35	99.58	99.77	99.98	100.04
Fa	0.9	33.6	0.9	43.5	0.2	38.2	2.4	35.8	0.6	37.6	0.7	37.5	0.5	34.8	0.5	34.7

	GRV 020137		GRV 020104		GRV 020169		GRV 052191		GRV 050009		Julesburg		Dimmitt		GRV 050016	
Na_2O	-	0.03	0.04	0.03	-	0.03	0.01	0.03	-	-	-	-	-	-	-	0.01
K_2O	-	0.01	0.04	-	-	0.01	0.03	-	0.01	-	-	-	-	-	-	-
Cr_2O_3	0.07	0.03	0.15	-	0.07	0.01	0.10	0.10	0.11	0.05	0.07	0.25	0.05	0.03	0.19	0.05
MgO	56.35	33.70	55.78	33.06	53.99	31.20	54.86	28.04	55.51	41.18	53.35	30.16	56.18	37.37	54.85	35.10
CaO	0.69	-	0.51	0.02	0.15	0.03	0.67	0.27	0.42	0.05	0.35	0.02	0.72	0.11	0.25	0.10
MnO	-	0.57	0.01	0.44	0.05	0.44	-	0.49	-	0.46	0.01	0.45	-	0.46	-	0.28
Al_2O_3	0.32	0.05	0.38	0.04	0.06	0.04	0.24	0.08	0.24	0.12	0.17	0.04	0.29	0.04	0.17	0.05
TiO_2	0.13	0.03	0.11	0.04	0.06	0.04	0.12	0.02	0.06	0.07	0.03	0.05	0.12	0.05	0.05	0.03
FeO	0.39	27.47	0.62	30.09	2.29	30.50	1.09	34.61	1.31	19.20	2.94	30.42	0.51	23.97	1.69	25.70
SiO_2	41.30	37.73	41.95	36.49	42.81	37.53	42.12	35.55	41.47	38.43	42.24	38.36	41.98	37.82	42.78	38.37
Total	99.25	99.62	99.58	100.20	99.49	99.82	99.22	99.20	99.13	99.55	99.16	99.75	99.84	99.85	99.97	99.69
Fa	0.4	31.4	0.6	33.8	2.3	35.4	1.1	40.9	1.3	20.7	3.0	36.1	0.5	26.5	1.7	29.1

	GRV 052722		GRV 020034		GRV 020054		GRV 020105		GRV 022921		GRV 020036		GRV 022455		GRV 021528		GRV 022410	
Na_2O	0.01	-	0.01	-	0.05	0.04	0.01	0.01	0.01	0.02	0.01	-	0.01		0.01		-	
K_2O	0.03	0.01	0.02	0.01	0.01	0.01	0.01	-	0.02	0.01	-	-	0.02		-		0.02	

Cr_2O_3	0.10	-	0.04	-	0.25	-	0.43	0.02	0.02	0.02	0.13	0.02	-	0.01	0.08
MgO	54.85	36.15	50.85	36.08	51.97	34.13	55.61	31.26	50.77	40.59	51.67	37.63	37.93	40.68	41.40
CaO	0.67	0.02	0.04	0.02	-	0.02	0.15	0.01	0.04	-	0.19	-	0.02	0.09	0.01
MnO	0.08	0.45	0.22	0.45	0.13	0.49	0.09	0.42	0.22	0.45	0.03	0.40	0.41	0.39	0.45
Al_2O_3	0.25	0.06	0.04	0.06	0.17	0.05	0.03	0.05	0.04	0.04	0.12	0.05	0.08	0.04	0.08
TiO_2	0.12	0.10	0.03	0.10	0.08	0.05	0.03	0.03	0.03	0.20	0.07	0.04	0.06	0.02	0.13
FeO	1.62	25.70	6.68	25.46	5.33	27.88	1.32	31.50	6.70	20.89	5.72	24.68	21.88	20.13	18.59
SiO_2	42.23	37.37	41.72	37.37	41.71	37.61	41.74	36.44	41.70	38.09	42.17	37.61	39.07	38.76	39.20
Total	99.95	99.86	99.63	99.54	99.69	100.28	99.41	99.74	99.54	100.30	100.11	100.43	99.47	100.13	99.95
Fa	1.6	28.5	6.9	28.4	5.4	31.4	1.3	36.1	6.9	22.4	5.8	26.9	24.5	21.7	20.1

-: not detected.

Table 6. Electron microprobe data (wt %) of the most Mg-rich and Fe-rich low-Ca pyroxene grains in every sample

	Semarkona		Krymka		GRV 020035		GRV 020032		GRV 020006		Sharps		Chainpur		GRV 020011		GRV 020137	
Na_2O	0.02	0.04	-	0.01	-	-	0.03	0.24	-	0.12	0.02	0.05	-	0.02	0.01	0.02	0.01	0.17
K_2O	0.01	0.02	0.02	-	0.01	0.01	0.03	0.03	-	-	-	-	-	-	-	-	-	-
Cr_2O_3	0.38	0.76	0.41	0.70	0.01	0.70	0.44	0.91	0.29	0.69	0.35	0.34	0.37	0.82	0.42	0.71	0.04	0.83
MgO	37.83	25.84	38.90	24.98	39.61	23.75	37.41	21.69	38.24	22.07	36.76	29.76	39.01	26.35	39.44	24.32	38.58	21.95
CaO	0.95	0.66	0.47	0.63	0.12	0.86	0.41	2.28	0.37	0.08	1.43	0.18	0.33	0.63	0.33	1.07	0.26	2.29
MnO	0.05	0.58	0.05	0.24	0.06	1.04	0.06	0.82	0.01	0.87	0.06	0.41	0.01	0.63	0.05	0.68	0.14	0.77
Al_2O_3	1.05	0.39	0.76	0.53	0.19	0.28	0.87	1.40	0.77	0.26	1.34	0.15	0.55	0.28	0.42	0.27	0.23	0.41
TiO_2	0.23	0.03	0.21	0.03	0.06	0.06	0.17	0.14	0.19	0.06	0.25	0.04	0.10	0.05	0.08	0.07	0.04	0.12
FeO	0.83	18.42	1.13	19.09	0.19	18.99	1.38	17.65	0.60	22.05	0.76	14.06	0.75	16.80	0.93	19.59	0.37	19.51
SiO_2	58.18	53.56	57.60	53.33	59.65	54.02	58.34	54.85	58.79	53.25	58.76	54.74	58.40	53.63	58.10	53.24	59.68	54.02
Total	99.53	100.30	99.53	99.52	99.90	99.72	99.14	99.99	99.24	99.43	99.72	99.73	99.52	99.21	99.78	99.97	99.35	100.06
Fs	1.2	28.2	1.6	29.6	0.3	30.4	2.0	29.8	0.9	35.9	1.1	20.9	1.1	26.0	1.3	30.5	0.5	31.7
En	97.1	70.5	97.6	69.1	99.5	67.8	97.2	65.3	98.5	64.0	96.2	78.8	98.3	72.7	98.1	67.4	99.0	63.5
Wo	1.8	1.3	0.8	1.2	0.2	1.8	0.8	4.9	0.7	0.2	2.7	0.3	0.6	1.3	0.6	2.1	0.5	4.8
	GRV 020104		GRV 020169		GRV 052191		GRV 050009		Julesburg		Dimmitt		GRV 050016		GRV 052722		GRV 020034	
Na_2O	0.02	-	-	0.03	-	0.06	-	0.02	-	0.02	-	0.06	-	0.04	-	0.05	0.02	0.02
K_2O	-	-	-	0.01	-	-	0.01	-	0.01	-	-	0.02	0.03	0.01	0.03	0.01	0.06	-

Cr_2O_3	0.35	0.41	0.20	0.18	0.40	0.56	0.53	0.05	0.72	0.34	0.71	0.63	0.57	0.32	0.30	0.82	0.18	0.13
MgO	36.76	27.79	36.59	18.69	36.80	25.45	37.72	26.71	36.55	26.50	36.53	25.63	37.30	29.21	38.01	23.92	34.70	27.48
CaO	1.43	0.62	1.80	0.16	0.13	1.03	0.13	0.51	1.36	0.28	1.35	0.24	0.24	0.93	0.19	1.32	0.20	1.00
MnO	0.06	0.23	0.02	0.33	0.17	0.65	0.06	0.52	0.38	0.54	0.40	0.42	0.16	0.72	0.03	0.71	0.68	0.43
Al_2O_3	1.34	0.24	2.68	0.10	0.19	0.36	0.22	0.10	1.49	0.22	1.48	0.18	0.39	0.20	0.13	0.53	0.32	0.19
TiO_2	0.25	0.03	0.45	0.01	0.01	0.07	0.08	0.10	0.16	0.04	0.18	0.04	0.09	0.06	0.05	0.10	0.06	0.22
FeO	0.75	15.71	0.63	27.23	3.27	18.23	1.77	14.56	1.22	16.74	1.28	18.03	1.47	11.92	1.89	18.68	5.95	15.81
SiO_2	58.76	54.54	58.24	52.97	58.55	52.84	59.46	57.22	57.57	55.24	57.55	54.18	59.21	56.19	59.56	53.32	57.71	54.77
Total	99.71	99.56	100.62	99.71	99.51	99.24	99.97	99.79	99.46	99.91	99.49	99.41	99.47	99.60	100.19	99.45	99.89	100.05
Fs	1.1	23.8	0.9	44.8	4.7	28.1	2.6	23.2	1.8	26.0	1.9	28.2	2.2	18.3	2.7	29.7	8.7	23.9
En	96.2	75.0	95.7	54.8	95.0	69.9	97.2	75.8	95.7	73.4	95.6	71.4	97.4	79.9	97.0	67.7	90.9	74.1
Wo	2.7	1.2	3.4	0.3	0.2	2.0	0.2	1.0	2.6	0.6	2.5	0.5	0.5	1.8	0.3	2.7	0.4	1.9

	GRV 020054		GRV 020105		GRV 022921		GRV 020036		GRV 022455		GRV 021528		GRV 022410	
Na_2O	0.01	0.02	-	0.04	0.08	-	0.01	0.05	0.03	0.04	-	0.03	0.01	0.02
K_2O	-	0.01	0.03	0.01	0.01	-	-	0.01	-	0.02	-	0.02	-	0.01
Cr_2O_3	0.67	0.14	0.30	0.59	0.49	0.10	0.04	0.82	0.44	0.73	1.03	0.67	0.31	0.34
MgO	36.18	27.60	38.09	28.00	37.46	30.97	38.22	23.92	31.53	24.46	33.74	26.26	37.08	29.87
CaO	0.17	0.87	0.19	1.03	0.40	0.51	0.28	1.32	1.27	1.31	2.16	1.32	0.08	0.36
MnO	0.43	0.43	0.04	0.72	0.15	0.51	0.07	0.71	0.15	0.71	-	0.71	0.14	0.29
Al_2O_3	0.35	0.19	0.13	0.39	0.40	0.15	0.14	0.53	1.09	0.46	4.27	0.42	0.15	0.23
TiO_2	0.05	0.18	0.06	0.08	0.05	0.15	0.06	0.09	0.09	0.09	0.58	0.09	0.01	0.07
FeO	4.45	13.46	1.89	14.93	2.10	11.04	2.71	18.88	8.20	18.86	2.05	17.62	3.94	13.31
SiO_2	57.89	56.39	59.56	54.25	59.07	56.67	58.62	53.03	56.92	53.03	55.29	53.03	58.47	55.46
Total	100.20	99.28	100.27	100.04	100.20	100.10	100.14	99.34	99.72	99.71	99.11	100.17	100.19	99.96
Fs	6.4	21.1	2.7	22.6	3.0	16.5	3.8	29.9	12.4	29.4	3.2	26.7	5.6	19.9
En	93.3	77.2	97.0	75.4	96.2	82.5	95.7	67.5	85.1	68.0	92.6	70.8	94.2	79.5
Wo	0.3	1.8	0.3	2.0	0.7	1.0	0.5	2.7	2.5	2.6	4.3	2.6	0.1	0.7

-: not detected.

4 Discussion

4.1 Petrologic types

Extensive studies have been made over the last 30 years since Sears[2] first used TL sensitivity to subdivide petrologic types of type 3. Subdivision is used to identify the least metamorphosed chondrites and to indicate the intensity of thermal metamorphism. With increasing metamorphic grade: diffusion homogenizes Fe and Mg in olivine; the texture of metal within chondrules changes; Cr-rich phrase separates from ferroan olivines; and feldspar increasingly crystallizes during devitrification of glass and recrystallization of matrix.

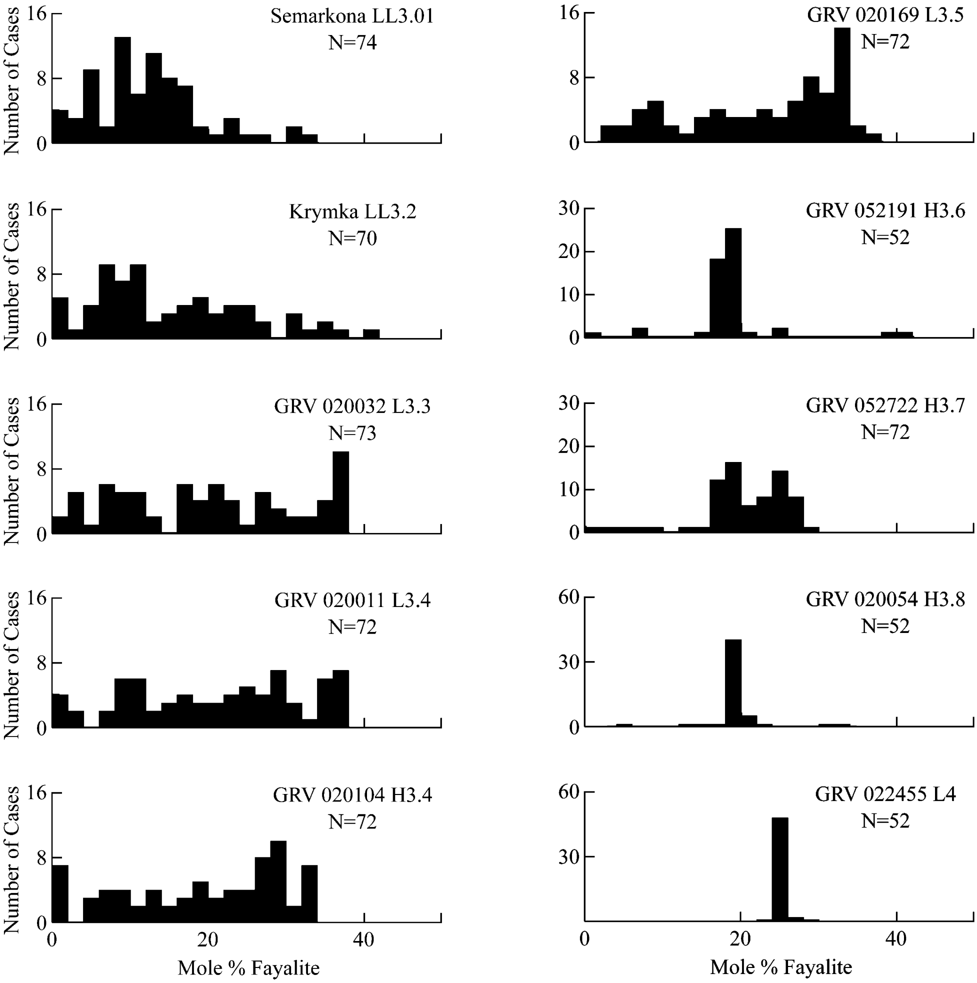

Fig 4 Histograms showing fayalite content of olivine in chondrites. The distribution becomes systematically narrower with increasing petrologic type. For type 3.6 to 4, the olivine has equilibrated at the mean fayalite value for the bulk meteorite.

We analyzed major element compositions (Mg, Si, Ca, Fe, O) of olivine and pyroxene grains of 25 UOCs and list silicate heterogeneity as CoV in table 3. The CoV values of Semarkona, Krymka, Sharps and Chainpur are all larger than 50, consistent with the assignments by Sears[10]. Sears suggested that TL sensitivity correlates with olivine heterogeneity because metamorphism homogenized the mafic silicate composition and also devitrified feldspathic glass to produce the TL phosphor, crystalline feldspar. However, the correlation breaks down in the most highly unequilibrated chondrites (type 3.0—3.4). It might be possible that homogenization of silicate compositions, which requires atomic diffusion over distances of several hundred μm, is a less facile process than devitrification of feldspathic glass which requires atom displacements over a few Å distance[10]. As seen in the table 3, the classification scheme by Sears[10] is a quite effective way to subdivide Antarctic meteorites.

In a given unequilibrated chondrite, the chemical variation of pyroxene is often greater than that of olivine. Pyroxene appears to be more resistant to thermal metamorphism than olivine. Even in type 4 chondrite (table 3), the CoV value of Fs could be as high as 24. For this reason, Grossman[19] suggested that type 4 chondrites with high PMD-Fs are presumably near the type 3 border and those with low PMD-Fs should be near the type 5 border.

4.1.1 Thermal history of Fe-Ni metal

The texture of Fe-Ni metal is a sensitive metamorphic indicator for chondrites of subtypes 3.00—3.2, since diffusion in metal is much faster than in oxides[20]. Semarkona chondrule metal shows pervasive fine-grained plessitic intergrowths. Kimura[9] observed many martensite in the primitive chondrite Acfer 094 (ungrouped carbonaceous chondrite, type 3.00) and pointed out that this primitive metal martensite was quenched in the solar nebula from high temperatures within chondrules before accretion to its parent body. Reisener[21] suggested that if the original taenite cools at >> 5 K/day, it transforms to martensite, which subsequently decomposes into a taenite + kamacite intergrowth during 1 year at temperatures as low as 573 K. That is to say, the plessitic intergrowths of metal in Semarkona chondrule interiors resulted from mild metamorphic heating of martensite under low temperature conditions in the parent body. During thermal metamorphism, plessite is transformed into intergrowths of coarser-grained kamacite and Ni-rich metal; grain size of Ni-rich metal increases and number density decreases. In Krymka (LL3.2), a few Ni-rich metal grains are several micrometers (Fig. 1b). Most metal grains are coarse-grained aggregates of kamacite and Ni-rich metal up to 15 μm. All other chondrites in this work show such coarse-grained aggregates with Ni-rich metal up to 40 μm, so we assign them to be type > 3.2.

4.1.2 Cr exsolution in olivine

In type 3.0 chondrites, olivine grains of type II chondrules are rich in Cr. In slightly metamorphosed types 3.1-3.2 chondrites, olivine grains show abundant homogeneous nucleation of a Cr-rich phase, producing fine, needle-like precipitates aligned along preferred crystallographic orientations. Apparently, continued heating to form higher-petrologic-type chondrites resulted in the coarsening of Cr-rich precipitates in olivine cores, presumably to minimize their surface energy, to the point where they formed much larger, equant grains (Fig. 2d). It is still not actually known whether the fine Cr-rich precipitates are chromite and the valence state and site occupancy of Cr in chondritic olivine are not well known[7, 22]. However, what is certain is that olivine grains in type I chondrules have low Cr contents and never show Cr exsolution in the cores, regardless of petrologic type.

4.1.3 Thermal effects in matrix

Semarkona, which was affected least by metamorphism, contains numerous sub-micrometer sulfides distributed in the extremely fine grained matrix (Fig. 3a). This was noted as a distinctive feature of type 3.0 by Dodd[4]. With increasing degree of thermal metamorphism, grain growth resulted in the formation of recrystallized matrix and caused coarsening of the remaining opaque matrix, accompanied by elemental migration (e.g. coalescence of the minute metallic FeNi and sulfide grains from the opaque matrix) and nucleation of feldspar in the recrystallized matrix. For type 4 chondrites (GRV 022455, GRV 021528, GRV 022410), the matrix consists entirely translucent to transparent crystals, although it can still be identified by grain size, morphology and location.

As mentioned above, nucleation and growth of plagioclase has been confirmed by measurements of TL sensitivity. The higher the TL sensitivity, the more abundant plagioclase in matrix. We did not observe any feldspar grains in the matrix of UOCs of types ≤ 3.3, which may be explained that they have not been annealed sufficiently to produce crystalline feldspar[10]. Above petrologic type ~ 3.4, matrix begins to show strong blue CL[3] and the alkali content again rises, indicating that secondary feldspar grains have begun to grow[7].

4.2 Chemical groups

The chemical classification scheme currently in common use is that of Van Schmus and Wood[1], mainly based on Fayalite content of olivine in ordinary chondrites. According to Van Schmus and Wood, the Fa values for H, L, LL are 16—20, 22-26, 27—31, respectively. However, olivine composition is not reliable for classifying the chemical groups of UOCs of types < 3.5[16], since Fe tends to be more reduced compared to that in the equilibrated chondrites. Consequently, we checked the chondrule size and the metal abundance to help to classify their chemical groups. As shown in table 3, mean Fa values of Semarkona, krymka, and chainpur are obviously inconsistent with their corresponding chemical groups, but they are very close to results of Dodd[4]. Results have proved that it is feasible to classify Antarctic meteorites by using EDS. In addition, we suggest that grain selection methods as in Dodd should always be used for classification of UOCs.

5 Conclusions

We studied the petrology and mineralogy of 25 unequilibrated ordinary chondrites (19 Chinese Antarctic meteorites). With increasing metamorphic grade: diffusion homogenized Fe and Mg in olivine; plessite in primitive chondrites was transformed into intergrowths of coarser-grained kamacite and Ni-rich metal; Cr exsolved from ferroan olivine, forming needle-like precipitates and then coarsened into equant chromite grains; and feldspar increasingly crystallized during devitrification of glass and recrystallization of matrix.

We subdivided 19 Antarctic meteorites into petrologic type 3.3—4 (3 for type 3.3, 3 for type 3.4, 1 for type 3.5, 2 for type 3.6, 2 for 3.7, 5 for 3.8, 3 for type 4). Results in this work indicate that the classification scheme proposed by Sears[10] is a quite effective way to subdivide Antarctic meteorites. In addition, we propose to revise chemical groups of GRV 020032, GRV 020104 to L, H, respectively and suggest that grain selection methods as in Dodd[4] are reasonable in classifying Antarctic meteorites.

Acknowledgments This work was supported by the National Natural Science Foundation of China (Grant No. 40773046 and 10621303), by Experimental Standardization and Sharing of the Polar Region Biological and Geological Sample Project (2005DKA21406), and by the Minor Planet Foundation of China.

References

[1] Van Schmus WR, Wood JA (1967): A chemical-petrologic classification for the chondrite meteorites. Geochimica et Cosmochimica Acta, 31: 747-765.

[2] Sears DWG, Grossman JN, Melcher CL *et al.* (1980): Measuring metamorphic history of unequilibrated ordinary chondrites. Nature, 287: 791-795.

[3] Sears DWG, DeHart JM, Hasan FA *et al.* (1990): Induced thermoluminescence and cathodoluminescence studies of meteorites. In: Coyne LM, McKeever SWS, Blake DF *et al.*, ed. Spectroscopic characterization of minerals and their surfaces, American Chemical Society, 190-222.

[4] Dodd RT, Van Schmus WR, Koffman DM (1967): A survey of the unequilibrated ordinary chondrites. Geochimica et Cosmochimica Acta, 31: 921-934.

[5] Zähringer J (1968): Rare gases in stony meteorites. Geochimica et Cosmochimica Acta, 32: 209-237.

[6] Huss GR, Keil K, Taylor G J (1981): The matrices of unequilibrated ordinary chondrites: Implications for the origin and history of chondrites, Geochimica et Cosmochimica Acta, 45: 33-51.

[7] Grossman JN, Brearley A J (2005): The onset of metamorphism in ordinary and carbonaceous chondrites. Meteoritics & Planetary Science, 40: 87-122.

[8] Kimura M, Nakajima H, Hiyagon H *et al.* (2006b): Spinel group minerals in LL3.00-6 chondrites: Indicators of nebular and parent body processes, Geochimica et Cosmochimica Acta, 70: 5634-5650.

[9] Kimura M, Grossman JN, Weisberg MK (2008): Fe-Ni metal in primitive chondrites: Indicators of classification and metamorphic conditions for ordinary and CO chondrites, Meteoritics & Planetary Science, 43: 1161-1177.

[10] Sears DW, Grossman JN, Melcher CL (1982): Chemical and physical studies of type 3 chondrites-I: Metamorphism related studies of Antarctic and other type 3 ordinary chondrites, Geochimica et Cosmochimica Acta, 46: 2471-2481.

[11] Wang DD, Miao BK, Lin YT (2005): Mineralogic-petrologic characteristic of meteorites and their classification. Chinese Journal of Polar Research, 17: 45-74.

[12] Gattacceca J, Rochette P, Denise M *et al.* (2005): An impact origin for the foliation of chondrites. Earth and Planetary Science Letters, 234: 351-368.

[13] Reisener R J, Goldstein JI (1999): Microstructural and chemical study of Fe-Ni metal inside Semarkona chondrules (abstract 1868). 30th Lunar and Planetary Science Conference. CD-ROM.

[14] Zanda B, Bourot-Denise M, Perron C *et al.* (1994): Origin and metamorphic redistribution of silicon, chromium, and phosphorus in the metal of chondrites. Science, 265: 1846-1849.

[15] Nagahara H (1984): Matrices of type 3 ordinary chondrites-primitive nebular records. Geochimica et Cosmochimica Acta, 48: 2581-2595.

[16] Weisberg MK, McCoy TJ, Krot AN (2006): Systematics and evaluation of meteorite classification. In: Meteorites and the Early Solar System II, edited by DS Lauretta and HY McSween Jr; University of Arizona, 19-52.
[17] Rubin AE, Scott ERD, Taylor GJ *et al.* (1983): Nature of the H chondrite parent body regolith: Evidence from the Dimmitt breccia. Journal of Geophysical Research, 88: A741-A754.
[18] Bischoff A, Sears DWG, Benoit PH *et al.* (1992): New type 3 ordinary chondrites from the Sahara Desert (abstract 107). 23th Lunar and Planetary Science Conference.
[19] Grossman JN, Rubin AE, Sears DWG (2009): The mineral composition and classification of high type 3 and type 4 ordinary chondrites (abstract 1679). 40th Lunar and Planetary Science Conference.
[20] Dean DC, Goldstein JI (1986): Determination of the interdiffusion coefficients in the Fe-Ni and Fe-Ni-P systems below 900°C. Metallurgical and Materials Transactions, 17A: 1131-1138.
[21] Reisener R, Meibom A, Krot AN *et al.* (2000): Microstructure of condensate Fe-Ni metal particles in the CH chondrite PAT 91546 (abstract 1445). 31st Lunar and Planetary Science Conference. CD-ROM.
[22] Ashworth JR (1979): Two kinds of exsolution in chondritic olivine. Mineralogical Magazine, 43: 535-538.